



**HAL**  
open science

## Size effects on exchange bias in sub-100 nm ferromagnetic–antiferromagnetic dots deposited on prepatterned substrates

Vincent Baltz, J. Sort, B. Rodmacq, B. Dieny, S. Landis

► **To cite this version:**

Vincent Baltz, J. Sort, B. Rodmacq, B. Dieny, S. Landis. Size effects on exchange bias in sub-100 nm ferromagnetic–antiferromagnetic dots deposited on prepatterned substrates. *Applied Physics Letters*, 2004, 84, pp.4923. 10.1063/1.1757646 . hal-01683687

**HAL Id: hal-01683687**

**<https://hal.science/hal-01683687>**

Submitted on 25 May 2019

**HAL** is a multi-disciplinary open access archive for the deposit and dissemination of scientific research documents, whether they are published or not. The documents may come from teaching and research institutions in France or abroad, or from public or private research centers.

L'archive ouverte pluridisciplinaire **HAL**, est destinée au dépôt et à la diffusion de documents scientifiques de niveau recherche, publiés ou non, émanant des établissements d'enseignement et de recherche français ou étrangers, des laboratoires publics ou privés.

## Size effects on exchange bias in sub-100 nm ferromagnetic–antiferromagnetic dots deposited on prepatterned substrates

V. Baltz, J. Sort,<sup>a)</sup> B. Rodmacq, and B. Dieny

SPINTEC (URA 2512 CNRS/CEA), CEA/Grenoble, 17 Av. Martyrs, 38054 Grenoble Cedex 9, France

S. Landis

LETI/D2NT, CEA Grenoble, 17 Av. Martyrs, 38054 Grenoble Cedex 9, France

(Received 5 February 2004; accepted 2 April 2004; published online 28 May 2004)

Exchange bias effects have been investigated in ferromagnetic (FM)–antiferromagnetic (AFM) square dots, with lateral sizes of 90 nm, sputtered on a prepatterned Si substrate. The magnetic behavior of the dots has been compared with that of a continuous FM–AFM bilayer with the same composition. Along the unidirectional direction, the dots exhibit square hysteresis loops and preserve an exchange bias field,  $H_E$ , of 70 Oe at room temperature, which is about 40% smaller than  $H_E$  in the continuous film. In addition, the distribution of blocking temperatures in the nanostructures is found to be shifted toward lower values with respect to that in the continuous film. These results can be interpreted assuming that the reduced lateral dimensions of the nanostructures impose some constraints on the formation and pinning of domain walls in the AFM layer. © 2004 American Institute of Physics. [DOI: 10.1063/1.1757646]

Exchange bias refers to the shift of the hysteresis loop, along the magnetic field axis, typically observed in exchange interacting ferromagnetic (FM)–antiferromagnetic (AFM) materials.<sup>1</sup> This loop shift is often accompanied by an enhancement of coercivity. The majority of models dealing with exchange bias consider that these effects originate from the formation of magnetic domains, either in the AFM<sup>2,3</sup> or in the FM layer.<sup>4</sup>

The study of exchange bias in nanostructures is interesting from both fundamental and technological points of view. From a fundamental point of view, the reduction of the lateral dimensions in FM–AFM systems can cause significant alterations on the domain structure of the layers, hence leading to substantial changes in the magnitudes of the exchange bias field,  $H_E$ , and coercivity,  $H_C$ , or in the asymmetry of the hysteresis loops.<sup>5–10</sup> From a technological point of view, the study of exchange bias in nanostructures is triggered by the tremendous increase in the areal density of magnetic data storage achieved during the last years. Reading heads are typically composed of spin valve or tunnel junction structures, in which FM–AFM exchange biased bilayers constitute an essential part.<sup>11</sup> In addition, it has been recently demonstrated that FM–AFM exchange interactions can be used to enhance stability of magnetic recording media.<sup>12,13</sup>

Although there exists a considerable number of studies on spin valve structures with micron or submicron dimensions,<sup>14</sup> the exchange bias effects arising from reduced sizes have been far less investigated.<sup>5–10</sup> Moreover, arrays of FM–AFM nanostructures in which both lateral dimensions are below 100 nm have not been studied so far. In addition, many of the FM–AFM submicron structures reported in the literature are obtained from the patterning of continuous bilayers. Postdeposition ion-etching processes typically cause

partial structural deterioration of the layers, which may result in pronounced kinks in the hysteresis loops. Hence, in nanostructures obtained by patterning continuous films, it is difficult to distinguish between the effects arising from the reduction of the lateral dimensions and those merely caused by structural deterioration.

In this letter, we investigate exchange bias effects in square FM–AFM dots sputtered on prepatterned Si substrates. A Si wafer was first patterned by conventional electron beam lithography and etching processes to form a  $1 \times 1 \text{ mm}^2$  array of Si square dots, with lateral sizes of 90 nm, height of 300 nm, and periodicity of 200 nm (see Fig. 1 inset). The magnetic material to study was then deposited on the Si nanodots. Hence, the nanopatterning of the magnetic material directly results from its deposition on the prepatterned wafer. This geometry is favorable to avoid the magnetic signal from the trenches, when measured by longitudinal Kerr effect. Namely, the pillars height to lateral spacing ratio, together with the low incidence angle ( $30^\circ$ ) results in pronounced shadowing effects which avoid the laser beam to reach the trenches. Further details on the nanostructuring technique have been published elsewhere.<sup>15</sup> A multilayer structure with composition Ta (5 nm)/Py (12 nm)/IrMn (5 nm)/Pt(2 nm) (where Py, i.e., permalloy, is FM and IrMn is AFM) was deposited, simultaneously, on unpatterned and patterned Si wafers by dc magnetron sputtering. To induce exchange bias, the as-grown samples were field cooled from  $T=450 \text{ K}$  (i.e., from above the blocking temperature of the system) using a field  $H_{FC}=2.4 \text{ kOe}$ , applied parallel to one of the edges of the square dots (see Fig. 1). Hysteresis loops were then measured, at room temperature, at several angles from the field cooling direction (arbitrarily taken as  $0^\circ$ ), using a longitudinal Kerr effect setup. The distribution of blocking temperatures in both the dots and the continuous film was also investigated.

<sup>a)</sup>Electronic mail: jordi.sort@uab.es

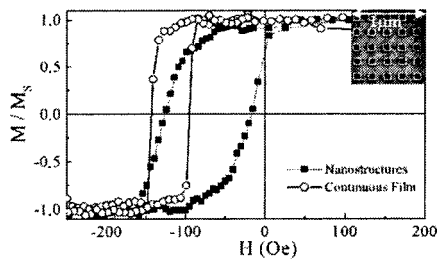


FIG. 1. Hysteresis loops of the continuous film and the array of dots, measured at room temperature by longitudinal Kerr effect along the field cooling direction after cooling from  $T=450$  K in the presence of a field  $H_{FC}=2.4$  kOe. The inset shows the SEM image of the dots.

Shown in Fig. 1 are the hysteresis loops of the continuous film and the array of dots, measured at room temperature along the field cooling direction. It can be seen that both hysteresis loops are rather square, with a remanence to saturation ratio,  $M_R/M_S$ , close to 1. Contrary to other studies on exchange bias in patterned elements,<sup>9,10</sup> no kinks or pronounced asymmetries are observed in the loops. This shape particularly differs from that of circular FM–AFM dots with very similar composition prepared by nanosphere lithography, where a significant reduction of  $M_R/M_S$  was observed due to the peculiar magnetic configurations, resembling vortex states, occurring during magnetization reversal.<sup>16</sup> However, arrays of small dots typically exhibit a broad switching field distribution (mainly attributed to the inhomogeneities among the dots).<sup>17</sup> This probably accounts for the slight tilt of the hysteresis loop observed in the nanostructures. It should be noted that, since the exchange bias is larger than the coercive field in these dots only one remanent state exists at zero field. This makes these exchange biased structures suitable as reference layer for spin-valves and tunnel junctions. Figure 1 also reveals that the magnitude of the exchange bias field,  $H_E$ , decreases from about 120 Oe (in the continuous film) to 70 Oe (in the nanostructures). The unidirectional character of exchange bias is revealed by the angular dependence of  $H_E$  for the continuous film and the nanostructures, shown in Fig. 2(a). The decrease of  $H_E$  in FM–AFM submicron dots has been sometimes reported in the literature.<sup>5,6,9,10</sup> This effect is probably related to some constraints imposed by the reduced lateral dimensions of the nanostructures on the formation of domain walls in the AFM. It can be argued that the presence of AFM domain walls allows a small surplus of magnetization at the FM–AFM interface, which couples with the FM, resulting in the unidirectional anisotropy.<sup>3,18</sup> Taking into account the values of the magnetic stiffness for IrMn ( $A_{\text{IrMn}} \sim 10^{-11}$  J/m<sup>3</sup>) and its magnetic anisotropy ( $K_{\text{IrMn}} \sim 1.8 \times 10^5$  J/m<sup>3</sup>), the domain wall width in IrMn,  $\delta_{\text{IrMn}}$ , can be roughly estimated to be  $\delta_{\text{IrMn}} \sim \pi (A_{\text{IrMn}}/K_{\text{IrMn}})^{1/2} \sim 25$  nm.<sup>19,20</sup> Hence, when the lateral dimensions of the nanostructures become of about the same order of magnitude as the AFM domain wall width, it is likely that some AFM domain walls, instead of being able to completely form (i.e., 180° domain walls), they may just be partially developed inside the nanostructures. These partial AFM domain walls may be less effectively pinned during magnetization reversal than complete domain walls in continuous FM–AFM films, thus leading to the observed decrease of  $H_E$ . In addition, a training effect was observed in

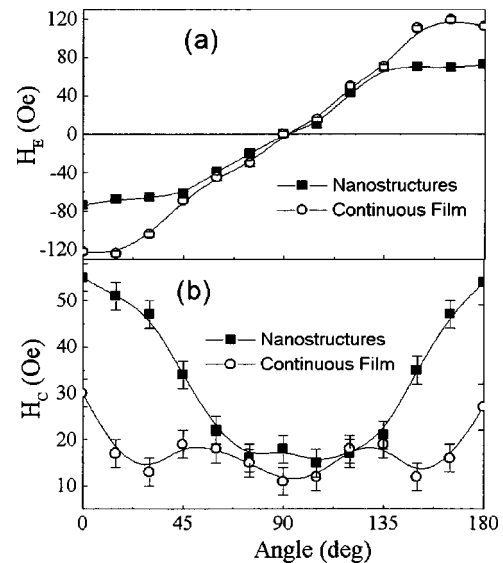


FIG. 2. Angular dependence of (a) the exchange bias field,  $H_E$ , and (b) the coercive field,  $H_C$ , measured at room temperature, for the field-cooled array of dots and the continuous film.

the nanostructures, i.e., the value of  $H_E$  was found to decrease by about 15% in the dots during the first three hysteresis loops, whereas no training effect was observed in the continuous film. Training effects are usually attributed to partial reorientation of AFM domain walls with each FM magnetization reversal.<sup>1</sup> Since this effect could only be observed in the nanostructures, this seems to confirm that, indeed, AFM domain walls may become less effectively pinned when reducing lateral dimensions of FM–AFM systems.

Contrary to  $H_E$ , the coercive field increases in the nanostructures along the unidirectional direction. Figure 2(b) shows the angular dependence of the coercive field for the continuous film and the dots. It is noteworthy that the coercive field of the dots when the hysteresis loop is measured at 90° from the field cooling direction is just slightly larger than that for the continuous film. Actually, an enhancement of  $H_C$  is commonly observed in patterned FM elements due to shape anisotropy or to the role of the edges of the nanostructures as barrier for the domain wall propagation.<sup>17</sup> This effect is mainly isotropic (i.e., the same for 0° or 90°). However, the  $H_C$  enhancement associated with FM–AFM exchange coupling in the dots is somewhat more pronounced than that of the continuous film for angles deviating as much as 45° from the field cooling direction. Hence, in our case, the large  $H_C$  enhancement in the nanostructures seems to originate, at least in part, from size effects on FM–AFM interactions. Indeed, if the domain walls in the AFM are less pinned than in the continuous film, the irreversibility associated with partial dragging of AFM spins during reversal of the FM in the dots can lead to the observed additional enhancement of  $H_C$  in the nanostructures. This result is particularly interesting since it can be used to enhance the magnetic stability of patterned media.

Exchange bias is known to typically vanish during heating at a temperature denoted as blocking temperature,  $T_B$ .<sup>1</sup> For single crystalline or relatively thick AFM layers, this temperature is usually close to the Néel temperature of the AFM,  $T_N$ . However, in some cases,  $T_B$  is much lower than

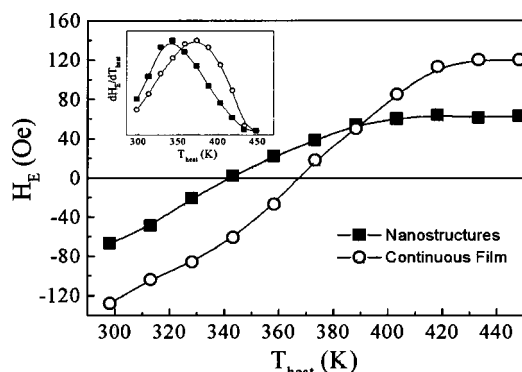


FIG. 3. Dependence of the exchange bias field,  $H_E$ , on the temperature ( $T_{\text{heat}}$ ) from which the dots and the continuous film, initially field cooled in  $H_{\text{FC}}=2.4$  kOe, have been field cooled in  $H_{\text{FC}}=-2.4$  kOe. All measurements have been performed at room temperature. Note that the lines are guides for the eye. Shown in the inset is the derivative  $dH_E/dT_{\text{heat}}$ .

$T_N$ . This effect is particularly pronounced when either the grain size of the AFM or the AFM layer thickness is relatively small.<sup>21–24</sup> In general, due to local variations in interface roughness or AFM crystallite sizes, a distribution of “local” blocking temperatures is encountered.<sup>1</sup> A standard procedure to study the  $T_B$  distribution is to progressively heat the sample to several temperatures,  $T_{\text{heat}} < T_B$ , and cool it in the presence of a field with opposite sign to the original cooling field.<sup>21,24</sup> Doing so, the magnitude of  $H_E$ , measured at room temperature, progressively decreases and changes sign. The relative change in  $H_E$  when cooling from two successive temperatures gives an idea of the number of FM–AFM regions with local blocking temperatures comprised between the two given temperatures.

The dependence of  $H_E$ , for the dots and the continuous film, on the temperature from which the samples have been field cooled in the negative field is shown in Fig. 3. As expected,  $H_E$  decreases with temperature in both cases. However, for the nanostructures,  $H_E$  is found to vanish at  $T_{H_E=0} \sim 345$  K, whereas  $T_{H_E=0} \sim 370$  K for the continuous film. It should be noted that, at  $T_{H_E=0}$ , half of the FM–AFM regions are coupled “positively” and half “negatively” or, in other words, half of the regions have local blocking temperatures above  $T_{H_E=0}$  and half below. In addition, the temperature at which  $H_E$  stabilizes after field cooling in a negative field (which corresponds to the maximum local blocking temperature), is found to be  $T_{B,\text{max}} \sim 400$  K for the dots and  $T_{B,\text{max}} \sim 430$  K for the continuous film. Shown in the inset of Fig. 3 is the derivative  $dH_E/dT_{\text{heat}}$ , which is typically used to represent the blocking temperature distribution in FM–AFM exchange coupled materials.<sup>21</sup> The derivative indicates that, indeed, the blocking temperature distribution for the dots is shifted toward lower values. This reduction in  $T_B$  should be taken into account in the design of devices in the deep sub-100 nm range.

Usually, finite size effects on FM or AFM particles (or thin films) are only observed when their sizes (or thickness) become very small (i.e., a few nanometers). At these sizes, the particles tend to lose their magnetic order due to the increasing role of thermal energy with respect to the anisotropy energy.<sup>25</sup> Reductions in the Curie and Néel temperatures have been experimentally reported<sup>26,27</sup> and theoretically

interpreted.<sup>28</sup> Our results seem to indicate that size effects on exchange bias start to appear at a lateral length scale somewhat larger than that at which the Curie or Néel temperature in the FM or AFM counterparts would be expected to reduce.<sup>25–28</sup> This effect may be interpreted as being due to an increasing role of thermally induced unpinning of AFM domain walls in the nanostructures. This hypothesis would be in agreement with the formation of partial domain walls in the FM–AFM dots, which could become less effectively pinned as temperature is increased.

This work was supported by the European Community through NEXBIAS Grant No. HPRN-CT-2002-00296. The authors acknowledge Stephane Auffret and Ursula Ebels for their discussions and technical assistance.

- <sup>1</sup>For recent reviews on exchange bias, see J. Nogués and I. K. Schuller, *J. Magn. Magn. Mater.* **192**, 203 (1999); A. E. Berkowitz and K. Takano, *ibid.* **200**, 552 (1999); R. L. Stamps, *J. Phys. D* **33**, R247 (2000); M. Kiwi, *J. Magn. Magn. Mater.* **234**, 584 (2001).
- <sup>2</sup>D. Mauri, H. C. Siegmann, P. S. Bagus, and E. Kay, *J. Appl. Phys.* **62**, 3047 (1987).
- <sup>3</sup>A. P. Malozemoff, *Phys. Rev. B* **35**, 3679 (1987).
- <sup>4</sup>M. Kiwi, J. Mejía-López, R. D. Portugal, and R. Ramírez, *Europhys. Lett.* **48**, 573 (1999).
- <sup>5</sup>M. Fraune, U. Rüdiger, G. Güntherodt, S. Cardoso, and P. Freitas, *Appl. Phys. Lett.* **77**, 3815 (2000).
- <sup>6</sup>J. Yu, A. D. Kent, and S. S. P. Parkin, *J. Appl. Phys.* **87**, 5049 (2000).
- <sup>7</sup>Y. Shen, Y. Wu, H. Xie, K. Li, J. Qiu, and Z. Guo, *J. Appl. Phys.* **91**, 8001 (2002).
- <sup>8</sup>A. Hoffman, M. Grimsditch, J. E. Pearson, J. Nogués, W. A. A. Macedo, and I. K. Schuller, *Phys. Rev. B* **67**, 220406 (2003).
- <sup>9</sup>Z. B. Guo, K. B. Li, G. C. Han, Z. Y. Liu, P. Luo, and Y. H. Wu, *J. Magn. Magn. Mater.* **251**, 323 (2002).
- <sup>10</sup>E. Girgis, R. D. Portugal, H. Loosvelt, M. J. Van Bael, I. Gordon, M. Malfait, K. Temst, C. Van Haesendonck, L. H. A. Leunissen, and R. Jonckheere, *Phys. Rev. Lett.* **91**, 187202 (2003).
- <sup>11</sup>B. Dieny, V. S. Speriosu, S. S. P. Parkin, B. A. Gurney, D. R. Wilhoit, and D. Mauri, *Phys. Rev. B* **43**, 1297 (1991).
- <sup>12</sup>K. Liu, J. Nogués, C. Leighton, H. Masuda, K. Nishio, I. V. Roshchin, and I. K. Schuller, *Appl. Phys. Lett.* **81**, 4434 (2002).
- <sup>13</sup>V. Skumryev, S. Stoyanov, Y. Zhang, G. Hadjipanayis, D. Givord, and J. Nogués, *Nature (London)* **423**, 850 (2003).
- <sup>14</sup>S. Tehrani, J. M. Slaughter, M. Deherra, B. N. Engel, N. D. Rizzo, J. Slater, M. Durlam, R. W. Dave, J. Janesky, B. Butcher, K. Smith, and G. Grynkwich, *Proc. IEEE* **91**, 703 (2003).
- <sup>15</sup>S. Landis, B. Rodmacq, B. Dieny, B. Dal’Zotto, S. Tedesco, and M. Heitzmann, *Appl. Phys. Lett.* **75**, 2473 (1999); S. Landis, B. Rodmacq, and B. Dieny, *Phys. Rev. B* **62**, 12271 (2000).
- <sup>16</sup>J. Sort, H. Glacysznska, U. Ebels, M. Giersig, J. Rybczynski, and B. Dieny, *J. Appl. Phys.* (in press).
- <sup>17</sup>For a recent review on the fabrication and properties of magnetic nanostructures, see: J. I. Martin, J. Nogués, K. Liu, J. L. Vicent, and I. K. Schuller, *J. Magn. Magn. Mater.* **256**, 449 (2003).
- <sup>18</sup>P. Miltényi, M. Gierlings, J. Keller, B. Beschoten, G. Güntherodt, U. Nowak, and K. D. Usadel, *Phys. Rev. Lett.* **84**, 4224 (2000).
- <sup>19</sup>D. Suess, T. Schrefl, W. Scholz, J. V. Kim, R. L. Stamps, and J. Fidler, *IEEE Trans. Magn.* **38**, 2397 (2002).
- <sup>20</sup>M. J. Carey, N. Smith, B. A. Gurney, J. R. Childress, and T. Lin, *J. Appl. Phys.* **89**, 6579 (2001).
- <sup>21</sup>S. Soeya, S. Nakamura, T. Imagawa, and S. Narishige, *J. Appl. Phys.* **77**, 5838 (1995).
- <sup>22</sup>T. Ambrose and C. L. Chien, *J. Appl. Phys.* **83**, 6822 (1998).
- <sup>23</sup>A. J. Devasahayam and M. H. Kryder, *J. Appl. Phys.* **85**, 5519 (1999).
- <sup>24</sup>C. Tsang and K. Lee, *J. Appl. Phys.* **53**, 2605 (1982).
- <sup>25</sup>For a recent review on magnetic properties of fine particle systems, see: X. Batlle and A. Labarta, *J. Phys. D* **35**, R15 (2002).
- <sup>26</sup>F. Huang, M. T. Kief, G. J. Mankey, and R. F. Willis, *Phys. Rev. B* **49**, 3962 (1994).
- <sup>27</sup>F. Bødker and S. Mørup, *Europhys. Lett.* **52**, 217 (2000).
- <sup>28</sup>W. H. Zhong, C. Q. Sun, B. K. Tay, S. Li, H. L. Bai, and E. Y. Jiang, *J. Phys.: Condens. Matter* **14**, L399 (2002).